

Closed-loop active vibration control of a typical nose landing gear with torsional MR fluid based damper

Sateesh B.[†] and Dipak K. Maiti[‡]

Department of Aerospace Engineering, Indian Institute of Technology, Kharagpur-721302, India

(Received January 25, 2008, Accepted December 4, 2008)

Abstract. Vibration is an undesirable phenomenon in a dynamic system like lightly damped aerospace structures and active vibration control has gradually been employed to suppress vibration. The objective of the current investigation is to introduce an active torsional magneto-rheological (MR) fluid based damper for vibration control of a typical nose landing gear. They offer the adaptability of active control devices without requiring the associated large power sources. A torsional damper is designed and developed based on Bingham plastic shear flow model. The numerical analysis is carried out to estimate the damping coefficient and damping force. The designed damper is fabricated and an experimental setup is also established to characterize the damper and these results are compared with the analytical results. A typical FE model of Nose landing gear is developed to study the effectiveness of the damper. Open loop response analysis has been carried out and response levels are monitored at the piston tip of a nose landing gear for various loading conditions without damper and with MR-damper as semi-active device. The closed-loop full state feedback control scheme by the pole-placement technique is also applied to control the landing gear instability of an aircraft.

Keywords: MR fluid; torsional damper; nose landing gear; full state feedback; pole placement.

1. Introduction

MR fluid dampers are, one of such new semi active control devices that are capable of generating the magnitude of controllable damping forces necessary for full scale applications, while requiring only a battery for power (Dyke and Spencer 1997). Changsheng *et al.* (2005) arranged disk-type MR fluid damper for rotor systems, it supplies the optimum supporting damping for every vibration mode in the rotor system and is very effective for attenuating and controlling the vibrations. Atray *et al.* (2003) were designed and manufactured an MR damper and installed in a 70-ton railcar for vibration control. Choi *et al.* (2003), investigated the use of a flow mode ER/MR landing gear shock strut, and concluded that the accelerations can be significantly attenuated using a sliding mode controller. Batterbee *et al.* (2007), developed dynamic model of an MR shock strut by retrofit an MR valve to an existing passive device to predict the landing gear impact performance and an investigation of the accuracy of the yield stress and viscosity predictions were presented which aims to validate the quasi steady performance of the MR valve. Lieh (1993) explores the use of semi

[†] Research Student, E-mail: sateesh_india@rediffmail.com

[‡] Associate Professor, Corresponding author, E-mail: dkmaiti@aero.iitkgp.ernet.in

active suspensions to control the dynamics of a full car model. Maiti *et al.* (2006) studied vibration control of dynamic systems using a semi-active MR-damper. Yao *et al.* (2001), developed a half - scale quarter car model setup including Bouc-Wen model of the MR damper and a semi-active control strategy was adopted to control the vibration of suspension system. Shen *et al.* (2006), investigated dynamical behavior of the semi-active suspension of the locomotive with magnetorheological (MR) damper, where the MR model is obtained based on experimental results. The simulation results show that the semi-active suspension of the locomotive with MR damper could lower the vibration of locomotive effectively almost as the active control. Dyke *et al.* (1996) presented the clipped linear optimal control law that has been shown effective for MR damper. Zhu *et al.* (2003) applied stochastic optimal semi-active control strategy for MR/ER damper. Kuo *et al.* (1997) designed lead compensator with the most common feedback system and showed that the best overall system performance can be obtained for a rotating flexible structure, only by adjusting the gain. The closed loop state feedback control scheme by pole-placement technique is widely used in control literature. Pourzeynali *et al.* (2005) applied to study the control of the flutter instability of suspension bridges, results shows that oscillations of the bridge come down to almost zero value within a few seconds. Yoshioka *et al.* (1999) developed active micro-vibration control system by the pole assignment method using genetic algorithm. This system showed good vibration control performance when applied to dynamic systems. The pole assignment techniques to modify the dynamic response of linear systems are among the most studied problems in modern control theory (Kautsky and Nichols 2004).

This study presents the design, fabrication and testing of a torsional type MR fluid based damper and its implementation to nose landing gear. It is observed from literature that the MR dampers are used as shock absorber to suppress the vertical vibration. In this present research, the effect of the torsional MR damper on longitudinal, lateral and torsional dynamics of nose landing gear is studied to suppress undesirable vibration. Open loop response analysis of nose landing has been carried out due to ground frictional force and response levels are monitored at the piston tip for various loading conditions. It is observed that the imbalance loading condition is the source of vibration. The response levels are also monitored with MR-damper as semi-active device. The closed-loop response is carried out using full state feedback control scheme by the pole-placement technique to control the landing gear instability of an aircraft.

2. Modeling and fabrication of a Torsional MR damper

2.1 MR damper modelling

In order to investigate the dynamical behavior of the MR system, the first and most important thing is to model the MR device. Several mechanical models such as Bingham Plastic model and Bouc-Wen model have been proposed for MR/ER dampers. For a steady and fully developed flow, the shear resistance of MR fluids may be derived using Bingham Plastic shear model (Zhu *et al.* 2004) as

$$\tau = \mu\dot{\gamma} + \tau_y(H)\text{sgn}(\dot{\gamma}) \quad (1)$$

where τ is the shear stress in the fluid, μ is the Newtonian viscosity independent of the applied magnetic field, $\dot{\gamma}$ is the shear strain rate, τ_y is the yielding shear stress controlled by the applied field H .

The dynamic behaviour of the damper and effective force-displacement and force-velocity curves are generated based on the following numerical model as reported in literature (Maiti Dipak *et al.* 2006) i.e.,

$$\text{Torsional force} \quad T_d = [(F_{dy, \max} - F_{dy, \min})I/I_{\max}] \text{sign}(U) \quad (2)$$

where I - applied current in coil, I_{\max} - maximum current, U - relative velocity of the piston, $F_{dy, \min}$ - friction force of the bearing, $F_{dy, \max}$ - maximum force due to the magnetic field including bearing force.

2.1.1 MR damper design

The schematic diagram and the cross sectional details of the torsional type MR Fluid damper as shown in Fig. 1. The variables considered are controllable variables i.e., magnetic field, current, force etc. and uncontrollable variables are called i.e., geometric and constructional parameters which include geometric parameters, coil dimensions etc.

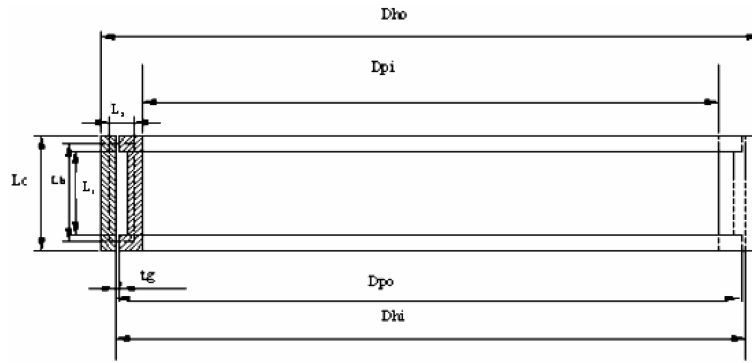


Fig. 1 Schematic of Torsional damper

Where

D_{hi} - Inner diameter of housing	D_{h0} - Outer diameter of housing
D_{pi} - Inner diameter of piston	D_{p0} - Outer diameter of piston
t_g - Gap between cylinder and piston	L_p - Total pole length ($L_c - L_i$)
L_c - Core length of magnetic path	L_i - Length of magnetic path through core
L_h - Length of magnetic path through housing	

The applications of controllable fluid are designed based on three modes of fluid interaction, which include a valve mode, a direct shear mode, and a squeeze film mode. In the present study we choose the direct shear mode operation and damping force estimated as follows

$$\text{Yield strength of the MR fluid } \tau_y = \alpha B \quad (3)$$

$$\text{Total pressure drop due to the field dependent yield stress } \Delta P = \frac{c \tau_y L_p}{t_g} \quad (4)$$

$$\text{Damping force } F = \pi D_{hi} L_p \Delta P \quad (5)$$

$$\text{Torsional moment required to break the magnetic chain } T_d = F * R \quad (6)$$

where R is the radius (arm length), B is the magnetic flux density. From literature (Maiti Dipak *et al.* 2006), α is the material constant (80 KPa/T) and c is a parameter whose value is 2.1. After fixing all the parameters described above, it is required to design the magnetic circuit.

2.1.2 Design of magnetic circuit

The task is to design a magnetic circuit (the path of the magnetic flux) and to estimate the required amp-turns (NI) as per the following design procedure (Maiti Dipak *et al.* 2006)

1. Determine H_f from the B-H curve of the MR fluid for given B_f (0.61 Tesla) as shown in Fig. 2.

2. The total magnetic induction flux is given by $\Phi = B_f A_f$ (9)

3. Determine B_s using continuity principle i.e., $\Phi = \Phi_{\text{fluid}} = \Phi_{\text{steel}} = \dots$ (8)

4. Determine H_s from the B-H curve of the steel as shown in Fig. 3 for designed

$$B_s = \frac{\Phi}{A_s} = \frac{B_f A_f}{A_s} \quad (9)$$

5. Using the Kirchoff's Law of magnetic circuits, determine the necessary number of amp-turns

$$NI = H_{sc} L_{sc} + H_c L_c * 2 + H_f t_g * 2 + H_h L_h \quad (10)$$

6. Based on the core length, calculate number of turns per length and number of layers required.

Where H_f , H_s is the Magnetic field density of MR fluid and steel, B_f , B_s is the magnetic field induction of MR fluid and steel, A_{sc} , A_{sh} is the area of core and housing for magnetic flux to flow, A_f , A_s is the surface area of MR fluid and remaining portion of steel area for magnetic flux to flow respectively, NI is the amp-turns for magnetic circuit, N is the number of turns of coil, I is the current.

2.2 Design task and geometry of MR damper

The design task is to estimate annular gap (t_g) and active pole length (L_p) in order to achieve the desired optimal damping force offered by the torsion damper with the application of varied magnetic field. Based on the literature (Maiti Dipak *et al.* 2006), in order to give a long life to the

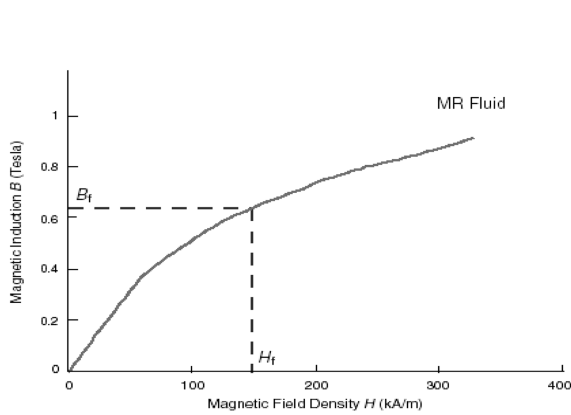


Fig. 2 B-H curve for MR fluid

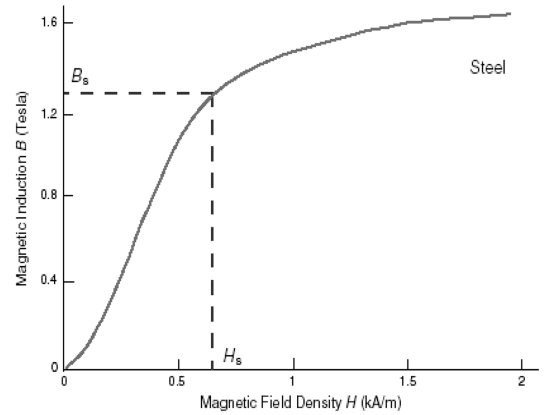


Fig. 3 B-H curve for steel

damper, which is subjected to cyclic loading during the course of its designed life, the annular gap (t_g) = 0.5 mm has selected. Pole length has been estimated from the design procedure as explained earlier. This damper was modeled with a cylinder of internal diameter (D_{hi}) and piston head diameter (D_{po}) works out to be ($D_{hi} - 2t_g$) mm and suitable thickness 4 mm is selected to satisfy the stability and strength criteria of the damper system. In the present design and analysis, damping force offered by the damper was estimated for $B_f = 0.61$ Tesla, $\alpha = 80$ Kpa/T and $\tau_y = 48.8$ KPa. Here value of B_f has selected from literature (Zhu 2005). Based on the design procedure explained earlier, the following geometric parameters are selected and geometrical model as shown in Fig. 4.

$D_{hi} = 116$ mm, $D_{po} = 115$ mm, $L_p = 8$ mm, $\Delta P_N = 1612800$ N/m²
 Surface Area = $4 * 22 * 2 * 10^{-6}$ m², Arm length = 0.058 m
 Damping Force for 10 pairs = 2838 N, Torsional Force = 164.60 N-m

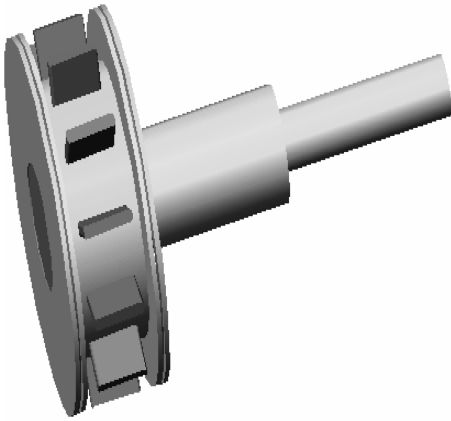


Fig. 4 Piston of MR damper with fins



Fig. 5 MR damper after winding

Magnetic circuit details:

NI = 144 turn-amperes	$N = 144$ turns	$I = 1$ amp
Core length = 15 mm	Number of Turns/gauge length = 72	
Number of layers = 2		

2.3 Experimental setup

Based on the design parameters, the MR damper is fabricated as shown in Fig. 5 and tested in the laboratory by using a Torsion testing machine (FTT-Model 20), which can conduct test on both metallic and non metallic materials of maximum torque capacity 200 N-m. The MR damper is fixed to the test machine as shown in Fig. 6. The experiments are conducted by angle-controlled mode and input current is given through the regulated DC power source, which is connected to the damper.

This machine applies a torque on the specimen held in its chuck and indicates a torsional load capacity. The regulated DC power supply source is used for different currents in the magnetic coil of the MR damper.



Fig. 6 Pictorial view of experimental setup

2.4 Results and discussion for MR damper

2.4.1 Dynamic behaviour of the damper and simulation results

To describe the behaviour of the damper, typical results of the force-displacement and force-velocity and force- time hysteresis loop for the sinusoidal excitation at frequency 1 Hz subjected to different applied currents are presented in Fig. 7. The typical values of the parameters in the Eq. (2) are $F_{dy,max} = 164.6$ N-m, $F_{dy,min} = 0$ N-m and $I_{max} = 1$ A.

The area enclosed by force vs. displacement loop represents mechanical energy, which has been dissipated, and the shape of the hysteresis loop determines the type of material response. The damper performance is often evaluated based on the force - velocity characteristics. The slope of the force - velocity line is known as the damping coefficient, C_d . It is observed that force- velocity line is bilinear and asymmetric, with different lower flux densities is that remnant magnetization of the magnetic circuit and MR material is diminished.

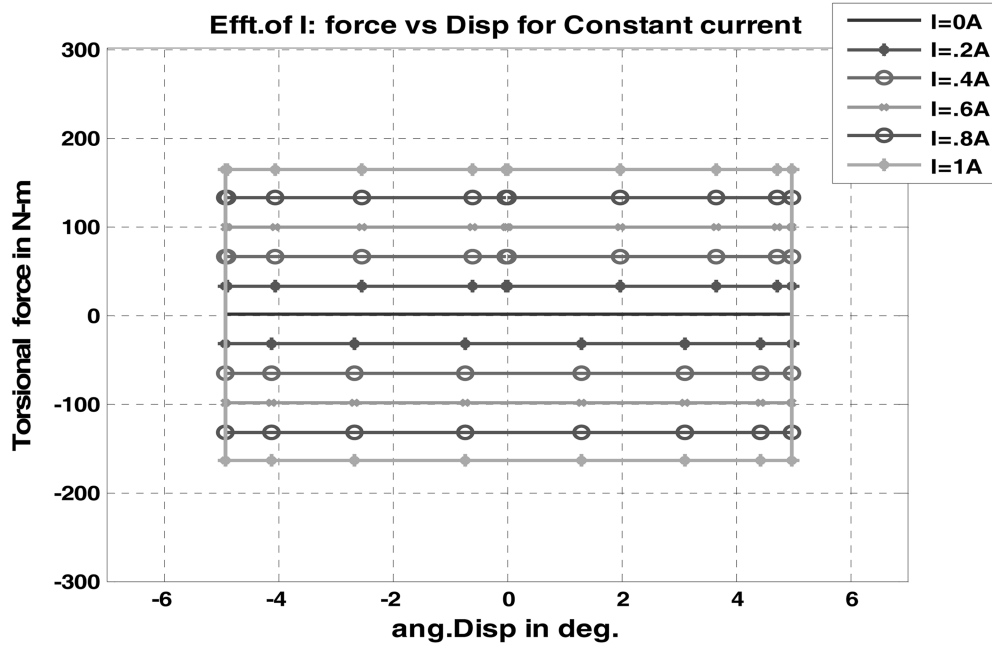
Fig. 7(a) shows the force – displacement loop, from which it is observed that force increases with the increase in the current. Fig. 7(b) shows the force vs. Angular velocity loop, from which it is observed that the damping force increases with the increase in the current and nature of the relationship is bilinear, which tells behaviour of the MR fluid is plastic in nature both in pre-yield (first slope) and post-yield (second slope) conditions. Fig. 7(c) illustrates the damping force is higher with the high input currents.

2.4.2 Energy dissipation and damping coefficient

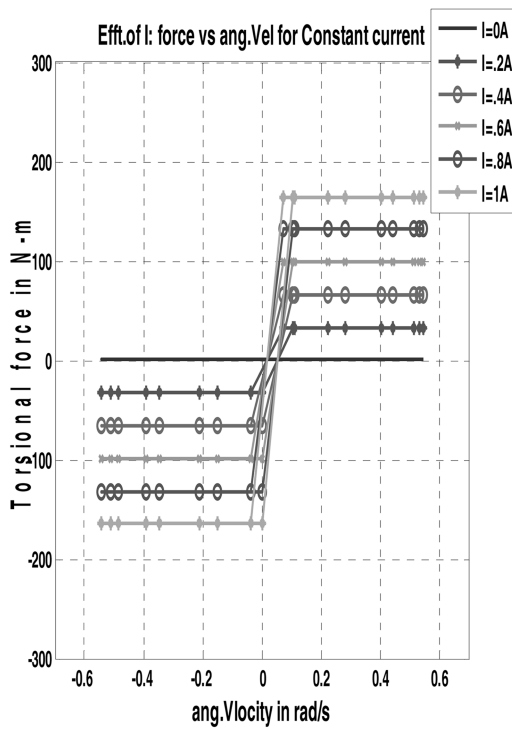
The energy dissipated by a damper over one vibration cycle is a measure of its damping capacity. In order to compare the damping performance of an MR damper with current, using Eq. (14) calculates the damping coefficient (C_d) for amplitudes 10^0 , 5^0 , 1^0 , 0.5^0 and variation with different input currents are plotted as shown in Fig. 8. It illustrates damping coefficient increases with decreasing amplitude.

2.4.3 Validation of experimental results with simulation results

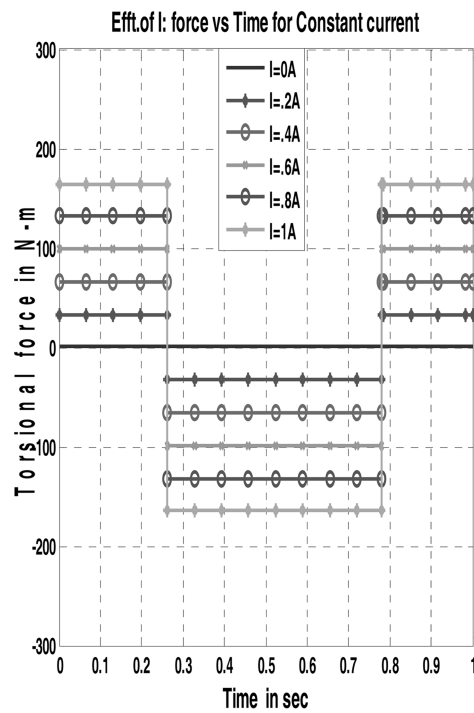
In the present analysis, the static experimental torsional damping force results are compared with the theoretical one. To examine the effect of damper in terms of damping force, the Torsional Force (T_d) - Angular Displacement (θ) and Torsional Force (T_d) - Time (t) predictions are compared with



(a) Force - Angular displacement



(b) Force - Angular velocity



(c) Force - Time

Fig. 7 $T_d - \theta$, $T_d - \omega$ and $T_d - T$ curves for $\theta_0 = 5^\circ$, $f = 1$ Hz at $I = 0(0.2)1$ A

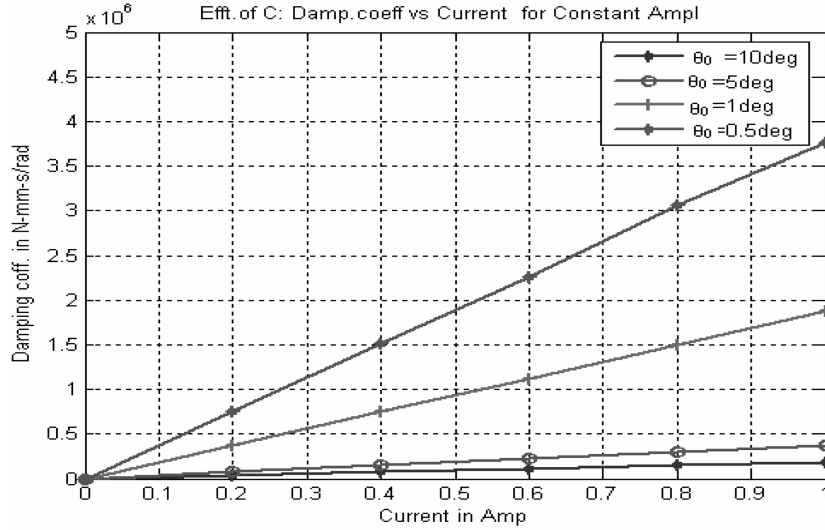


Fig. 8 Variation of damping coefficient C_d with input current for constant amplitudes

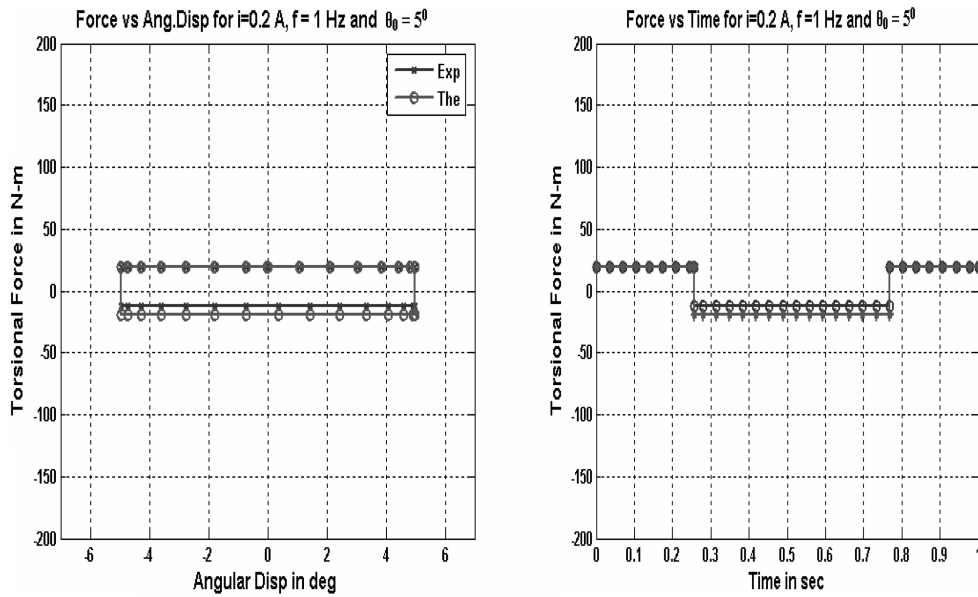
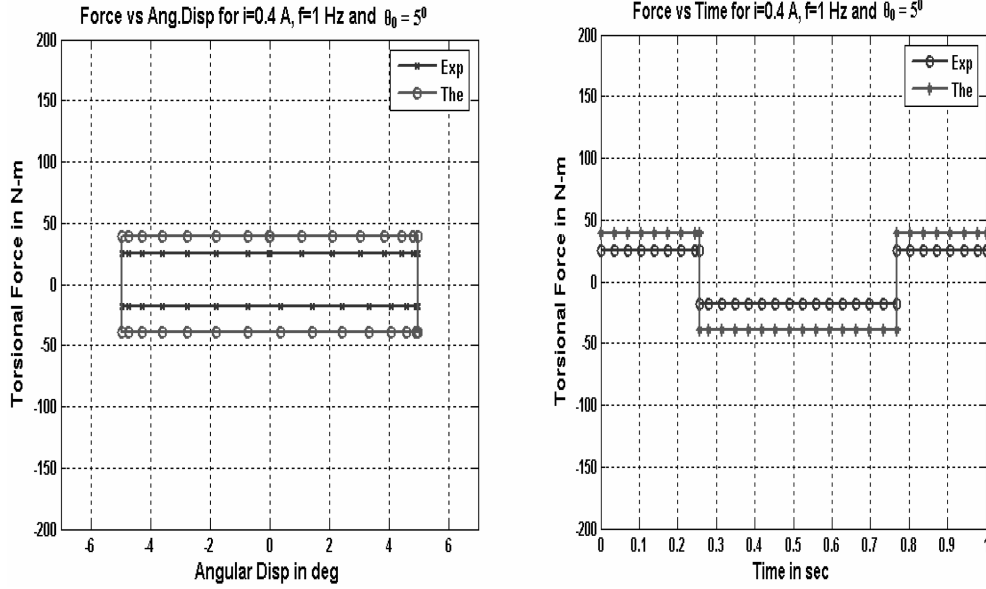


Fig. 9 $T_d - \theta$ and $T_d - t$ curves for $I = 0.2$ A, $f = 1$ Hz and $\theta_0 = \pm 5^\circ$

the simulated experimental results for the sinusoidal excitation of the frequency (f) 1 Hz and angular displacement amplitude (θ_0) of $\pm 5^\circ$ with input current (I) of 0.2 A and 0.4 A as shown in Figs. 9 and 10. The experimental results do not match with the theoretical one because the measured magnetic field is much lower than the designed one. The design of magnetic circuit has to be reviewed again and necessary corrections have to be implemented. But the theoretical study reveals the effectiveness of the designed MR damper.


 Fig. 10 $T_d - \theta$ and $T_d - t$ curves for $I = 0.4$ A, $f = 1$ Hz and $\theta_0 = \pm 5^\circ$

3. Mathematical formulation

3.1 Equation of dynamic system

In general, the equation of the motion of dynamic system, for example finite element modeling of structural systems is described in second order differential equation. So the undamped forced vibration equation of motion of the structural system is given as

$$[M]\{\ddot{x}\} + [K]\{x\} = [F] \quad (11)$$

where M , K and F are the mass, stiffness and external force vector of the system. Introducing modal transformation $x = [\phi]\{q\}$, the above system is converted into modal equation as given below

$$[\bar{M}]\{\ddot{q}\} + [\bar{K}]\{q\} = [\bar{F}] \quad (12)$$

By introducing damping in the system, the damped forced vibration equation of motion of the system is given as $[\bar{M}]\{\ddot{q}\} + [\bar{C}]\{\dot{q}\} + [\bar{K}]\{q\} = [\bar{F}]$ (13)

Where ϕ is the modal vector; q is the modal coordinate

$$[\phi]^T [M] [\phi] = \text{Modal mass matrix } [\bar{M}]; \quad [\phi]^T [K] [\phi] = \text{Modal stiffness matrix } [\bar{K}];$$

$$[\phi]^T [F] = \text{Modal force matrix } [\bar{F}]; \quad [\phi]^T [C_d] [\phi] = \text{Modal stiffness matrix } [\bar{C}];$$

$$\text{Here torsional damping coefficient } (C_d) = \frac{E}{\pi \Omega \theta_0^2} \quad (14)$$

E is the dissipated energy calculated from force-displacement diagram i.e., area under the curve; Ω is the excitation frequency and θ_0 is the angular displacement amplitude.

C_d has calculated from the Eq. (14) which is explained in the Maiti Dipak *et al.* (2006)

3.2 State-space method

State-space method (Kashani 1989) is one of the most convenient to form of any dynamic system in first order. Finally, by choosing the modal coordinates as the state variables, the state equation can be written in the standard state-space form as follows

$$\{\dot{x}\} = [A]\{x\} + [B]u \quad (15)$$

in which the state vector $\{x\}$ is defined as

$$\{x\} = \begin{Bmatrix} q \\ \dot{q} \end{Bmatrix} \quad (16)$$

The state matrix $[A] = \begin{Bmatrix} [0] & [I] \\ -[\bar{M}]^{-1}[\bar{K}] & -[\bar{M}]^{-1}[\bar{C}] \end{Bmatrix}$ and the input matrix $[B] = \begin{Bmatrix} [0] \\ [\bar{M}]^{-1}[\bar{F}] \end{Bmatrix}$

where $[0]$ and $[I]$ are the zero and identity matrices respectively, u is an input vector

3.3 Design of control system by the pole placement technique

The main role of feedback control is to find a feedback gain which makes the closed-loop system stable, so that all closed-loop eigenvalues are placed in the left half of the complex plane, which control the characteristics of the response of the system. The closed-loop pole locations have a direct impact on time response characteristics such as rise time, settling time and transient oscillations. According to the second method of Liapunov stability analysis, for a system represented by Eq. (15), the open-loop stability without external input is determined by the eigenvalues of the following equation

$$\{\dot{x}\} = [A]\{x\} \quad (17)$$

If all eigenvalues of matrix $[A]$ have negative real part, the system is asymptotically stable. The eigenvalues of the matrix $[A]$ are called the poles of the original system. If any of these poles lie on the right half of the s plane, then the system is unstable. The stability of a linear closed-loop system can be determined from the location of the closed-loop poles in the complex s plane, in which s are the poles of the system. For a second-order control system, it is shown (Ogata 1992) that the poles can be written as

$$s = -\zeta\omega_n \pm i\omega_d \quad (18)$$

where $\omega_d = \omega_n\sqrt{1-\zeta^2}$, $i = \sqrt{-1}$, ω_d is the damped natural frequency. ζ is the damping ratio, ω_n is the undamped natural frequency (rad/s)

$$\text{Control force } \{u\} = -[G]\{x\} \quad (19)$$

Here $[G]$ is the feedback gain matrix (Kwon and Bang 2000, Ogata 1992, Karagülle1 *et al.* 2004) and $\{x\}$ is the state vector.

Substituting Eq. (19) into Eq. (15) gives

$$\{\dot{x}\} = ([A] - [B][G])\{x\} \quad (20)$$

Here, the eigenvalues of the matrix $([A]-[B][G])$ are the desired closed-loop poles (p) of the controlled system, which would replace the poles of unstable system.

It is noted that for a given system, the matrix $[G]$ is not unique, but depends on the desired closed-loop locations selected, which determine the decay of the response. In order to determine the gain matrix $[G]$ for a given system, the response characteristics of the control system (Stefan *et al.* 2002, Aldemir and Bakioglu 2001, Aldemir 2003) is to be studied for a number of cases and the best one is to be selected. In present case gain matrix $[G]$ is computed using place command in matlab i.e., $G = \text{PLACE}(A, B, p)$. In this system we have more parameters than the number of equations to be satisfied; the extra degrees of the freedom can be used for other purposes such as improving system robustness.

4. Finite element model of a nose landing gear

4.1 Landing gears

Conventionally, there are two landing gear systems for any aircraft. One of them will be forward of the centre of gravity (CG) of the aircraft called as 'nose landing gear', while the other one positioned at the aft of the CG, is known as 'main landing gear. The landing gear is one of the most stressed parts of an airframe and is designed for the full aircraft life cycle. The landing gear is

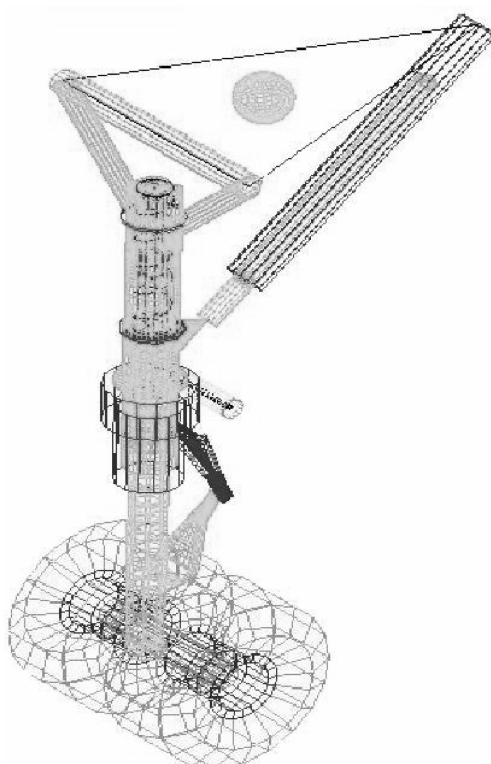


Fig. 11 Nose landing gear assembly

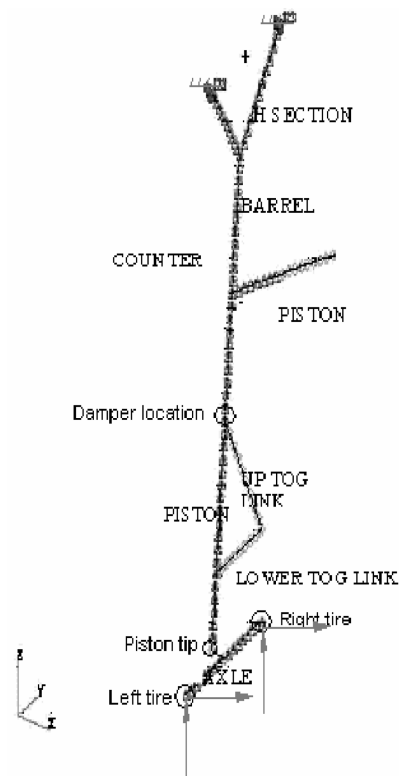


Fig. 12 FE Model of a landing gear

designed to absorb both vertical and horizontal energy during landing impact and also keep the aircraft in a stable position during ground maneuvers. Commercial aircraft should also provide a smooth ground ride during taxiing both for passenger comfort and safety reasons.

The main parts of the landing gear consist of a cylinder in which an oleo pneumatic shock absorber is positioned. Top end of the cylinder is connected to the fuselage of the aircraft, usually with two rigid bars. A steering mechanism with a rack and pinion arrangement, which permits the steering control by the pilot, is at the bottom end of the cylinder. The steering mechanism is connected with a piston, which can move to and fro in a cylinder in such a way that the diameter of the piston is made smaller than that of the cylinder. The toggle links are connected to the steering mechanism, which in turn will transfer the rotation to the axis of axle on which the tires are mounted. The conventional landing gear for large aircraft consists of a set of tires, sometimes a bogie. Fig. 11 shows realistic NLG.

4.2 Finite element analysis of a typical nose landing gear

The landing gear is one of the most essential in aircraft systems; it is a design driver for the entire aircraft configuration. A finite element model (Khulief 2001) of a nose landing gear (NLG) is shown in Fig. 12. The model is developed in MSC.NASTRAN using the pre/post processor. The NLG attachments to the fuselage are simulated as pin joints by fixing the translational degrees of freedom in the FE model. The fuselage is assumed to be rigid. The finite element model is developed based on the idealization using beam elements. The important members of the Nose Landing Gear assembly i.e., fork, barrel (housing), inner piston, piston, upper and lower toggle links, jack-piston, wheel axle, the link to the piston and the wheel axle, are simulated in the FE model with appropriate geometric properties. The normal mode analysis is performed to determine the natural frequencies and their mode shapes. The results of the free vibration analysis (first 5 frequencies and mode types) of the NLG are shown in Table 1.

Table 1 Modal properties of NLG

Mode No	Frequency ω_n (Hz)	Mode type
1	21.76	Lateral bending mode
2	31.10	Longitudinal Bending mode
*3	67.34	Torsional mode
4	93.02	Second lateral Bending mode
5	167.87	Second longitudinal and axle bending mode

*dominating mode because of torsional damper

4.3 Results and discussions

4.3.1 Open loop response analysis of NLG without and with MR damper

A response model of a nose landing gear is developed based on the above modal information. A nose landing gear shares some percentage (present case, it is assumed that 10%) of total aircraft weight. The response analysis is carried out with actual loading conditions on both left and right tires (i.e., vertical self weight of aircraft and horizontal frictional load acting for the whole duration)

Table 2 Acceleration response at piston tip of NLG without and with damper

Loading conditions on tires	RMS acceleration, g	
	without damper	with damper
Balance (50-50%)	0.5595	0.5504
Imbalance1 (45-55%)	1.4426	0.8965
Imbalance2 (40-60%)	3.1505	2.1664

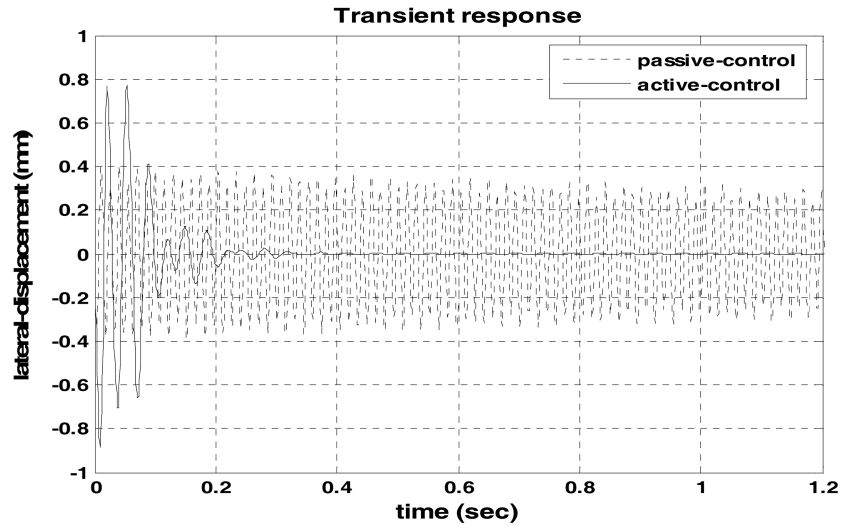
i.e., balanced loading condition also called equal sharing of load by two tires (i.e., 50%-50%) and imbalanced loading condition also called unequal sharing of load by two tires (i.e., 45%-55% and 40%-60%) without damper and with MR damper (varying the current through the coil) and results are tabulated in Table 2. In balanced loading case without damper, the RMS acceleration at piston tip in lateral direction is 0.5595 g. The above loading condition is an ideal one. In reality, the loading may not be perfectly balanced. In imbalance loading, it shows 1.4426 g with 45%-55% load sharing and 3.1505 g with 40%-60% load sharing respectively. An acceleration level is high with imbalance loading compared to that of balanced loading. This indicates that imbalance loading is a source of vibration in a nose landing gear of an aircraft. After implementing the MR-damper there is a significant improvement in the reduction of acceleration.

4.3.2 Closed loop response using full state feedback control by the pole placement technique

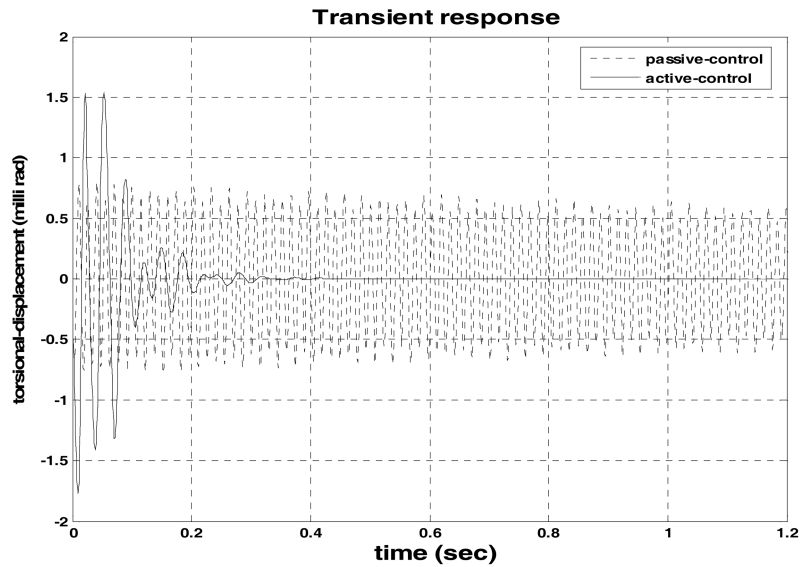
The feedback controller design needs system or plant characteristics as input, either in the form of transfer function or state space matrices. However, modern control concepts employ the state-space approach. In the present numerical study, the FE model of a nose landing gear (NLG) as shown in Fig. 12 is chosen. The structural system can be parameterised using stiffness, mass and damping matrices. Controller was designed using full state feedback control by the pole placement technique by giving velocity feedback (Preumont 1996) as described in section 3.3. The developed finite element model and control procedures are coded in MATLAB. Therefore, it is possible to carry out both structural and control analyses in the same platform. The free vibration analyses are performed and the results are shown in Table 2. From these results, for further parametric studies first three modes are considered in the analysis, because torsional (third) mode is the predominant mode in torsional damper application to NLG. The contribution of the other modes in the overall response of NLG is very less in comparison with the first three modes.

In order to perform the stability analysis, the results of the controlled and uncontrolled transient responses at piston tip of the landing gear was compared. Figs. 13(a) and (b) show the lateral and torsional displacement responses of the NLG respectively. It can be seen from the figures that the controlled response of the NLG decays with time. Here the open loop damping is 3.96%. In order to control the system response, the desired poles are selected at an active damping of 9%. Note that this value is selected by computer simulation in order to obtain a good controlled response. It is seen from the Fig. 13 that both lateral and torsional responses decay much faster and reached to almost zero value within a very short time.

Fig. 14 shows the uncontrolled and controlled frequency response. Figs. 14(a) and (b) show the variation of amplitude with frequency in lateral and torsional direction respectively. Interestingly, the comparison study shows that significant amplitude reduction of the system in both lateral and rotational direction are achieved.



(a) lateral-displacement vs. time



(b) torsional-displacement vs. time

Fig. 13 Controlled and uncontrolled transient responses at piston tip of NLG with imbalanced loading (40%-60%)

The control action needed to reduce the instability of system for imbalanced loading as shown in Fig. 15. Note that the applied control action is a torsional moment applied to the NLG. It is seen from the figure that the transient response is brought amplitude to almost zero value within 0.35 s. This control force shoots the damping force given by the torsional damper. But in order to stabilize quickly, the active damping coefficient has to increase, but control force increases with increasing damping coefficient. Figs. 16(a) and (b) show the control action required for 15% and 20% of damping value respectively. It is observed that, the control force required is 169 N-m for 15%

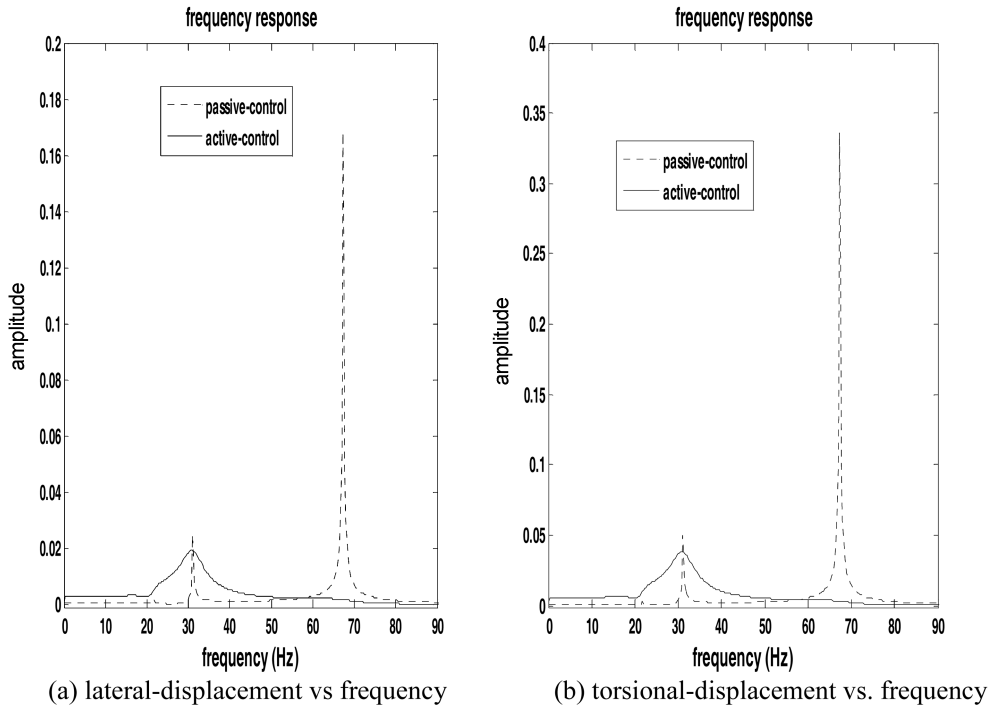


Fig. 14 Controlled and uncontrolled frequency responses with imbalanced loading (40%-60%)

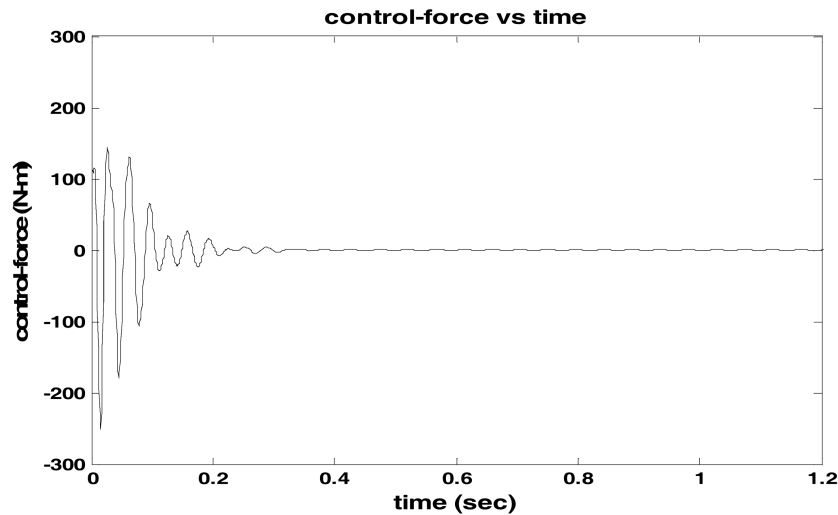


Fig. 15 Control-force vs. time response at $\zeta = 0.09$ with imbalanced loading (40%-60%)

damping, but it settles at 0.2 s and 205 N-m for 20% but it settles at 0.12 s.

For the same control effect, in order to reduce the control force, fix the damper just above the steering (i.e., the present location as shown in Fig. 12). Fig. 17 shows the control action required at $\zeta = 0.20$ i.e., control force is 196 N-m, but it stabilize the NLG at 0.12 s only. Figs. 18(a) and (b) show the controlled transient response in lateral and rotational direction. This indicates that effectiveness

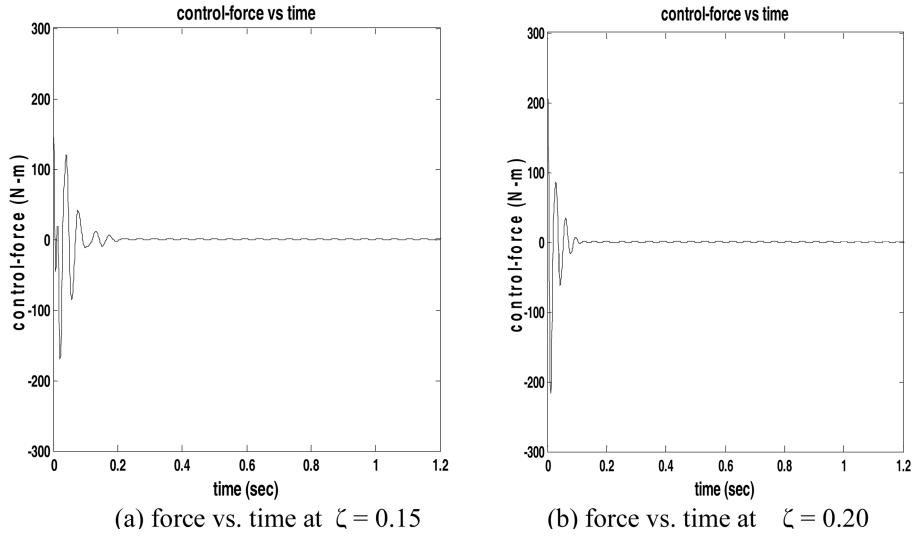


Fig. 16 Control-force vs. time responses with imbalanced loading (40%-60%)

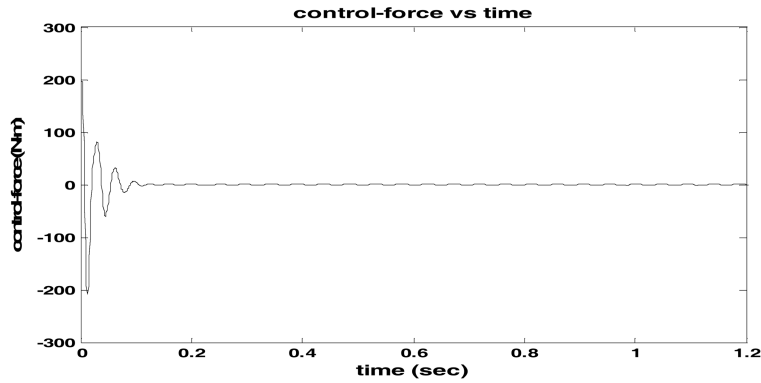


Fig. 17 Control-force vs. time responses at $\zeta = 0.20$ with damper just above the steering

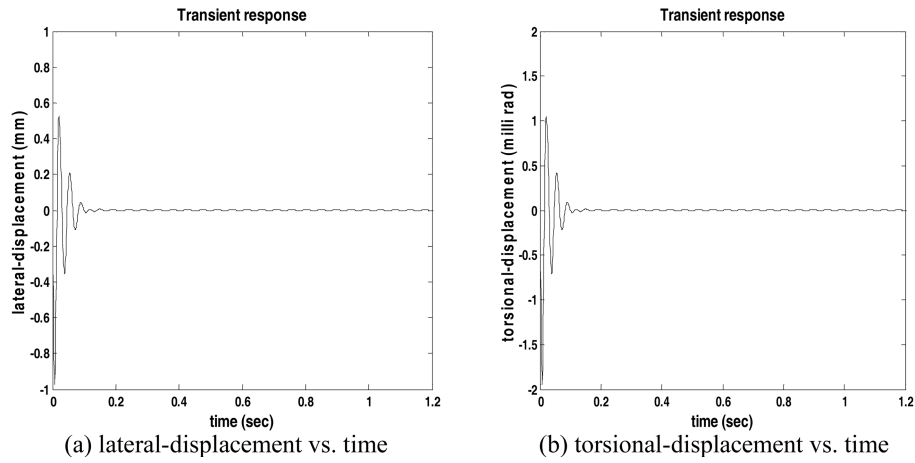


Fig. 18 Controlled transient response at $\zeta = 0.20$ with damper just above the steering and imbalanced loading (40%-60%)

of the velocity feedback control by the pole-placement technique to stabilize the NLG instability.

5. Conclusions

A unique active torsional MR fluid based damper is designed, fabricated and tested. The experimental results are compared with the theoretical predictions. A typical FE model of a Nose landing gear is developed to study the vibration characteristics due to ground excitation. Open loop response analysis has been carried out and the response levels are monitored at the piston tip of a nose landing gear for various loading conditions without MR damper and with MR-damper as semi-active device. It is observed that the imbalanced loading condition is the main source of excessive vibration and can be reduced with the application of MR damper. An efficient closed-loop full state feed back control scheme by the pole-placement technique is presented for active control of landing gear instability of an aircraft. Results demonstrate that the transient response is brought amplitude to almost zero value within a short span of time. This indicates the effectiveness of the pole-placement technique to stabilize the NLG instability. Finally we can conclude that torsional MR damper is a good semi-active candidate for vibration control and the proposed control strategy significantly reduces the decay time to bring down the transient response to almost zero value within a short period to control instability of an aircraft.

References

- Aldemir, U. (2003), "Modified disturbance rejection problem", *Comput. Struct.*, **81**, 1547-1553.
- Aldemir, U. and Bakioglu, M. (2001), "Active structural control based on the prediction and degree of stability", *J. Sound Vib.*, **247**(7), 561-576.
- Atray, V.S. and Roschke, P.N. (2003), "Design, fabrication, testing, and fuzzy modeling of a large magnetorheological damper for vibration control in a railcar", *Proceedings of the 2003 IEEE/ASME Joint Rail Conference*, Chicago, Illinois.
- Batterbee, D.C., Sims, N.D., Stanway, R. and Wolejsza, Z. (2007), "Magnetorheological landing gear: 1. A design methodology", *Smart Mater. Struct.*, **16**, 2429-2440, doi:10.1088/0964-1726/16/6/046.
- Batterbee, D.C., Sims, N.D., Stanway, R. and Wolejsza, Z. (2007), "Magnetorheological landing gear: 2. Validation using experimental data", *Smart Mater. Struct.*, **16**, 2441-2452, doi:10.1088/0964-1726/16/6/047.
- Choi, Y.T. and Wereley, N.M. (2003), "Vibration control of a landing gear system featuring electrorheological/magnetorheological fluids", *J. Aircraft*, **40**, 432-439.
- Dyke, S.J. and Spencer, B.F. Jr (1997), "A comparison of semi-active control strategies for the MR damper", *Proceedings of the IASTED International Conference*.
- Dyke, S.J., Spencer, B.F., Sain, M.K. and Carlson, J.D. (1996), "Modeling and control of magneto-rheological dampers for seismic response reduction", *Smart Mater. Struct.*, **5**, 565-75.
- Karagüllel, H., Malgacal, L. and Oktem, H.F. (2004), "Analysis of active vibration control in smart structures by ANSYS", *Smart Mater. Struct.* 13, online at stacks.iop.org/SMS/13/661.
- Kashani, R. (1989), "State-space formulation of linear systems", Ph.D. article available online: www.deicon.com/vib_tutorial/ssmodel_pdf.pdf
- Kautsky, J. and Nichols, N.K. (2004), "Robust pole assignment in linear state feedback", *Int. J. Control*, **41**, 1129-1155.
- Khulief, Y.A. (2001), "Active modal control of vibrations in elastic structures in the presence of material damping", *J. Comput. Meth. Appl. Mech. Eng.*, **190**, 6947-6961.
- Kuo, C.J. and Lin, S. (1997), "Lead with closed-loop system compensation of a radically rotating elastic rod attached to a rigid body Part I: A unified approach to the design of linear control system", *Comput. Math. Appl.*

- Kwon, Y. and Bang, H. (2000), "The FEM using Matlab", second edition, CRC press.
- Lieh, J. (1993), "Semiactive damping control of vibrations in automobiles", *J. Vib. Acoust.*, **115**(3), 340-343.
- Maiti Dipak, K., Shyju, P.P. and Vijayaraju, K. (2006), "Vibration control of mechanical systems using semi-active MR-damper", *Smart Struct. Syst.*, **2**(1), 61-805.
- Ogata, K. (1992), "Modern control engineering", Prentice Hall of India (P) Ltd., New Delhi.
- Pourzeynalia, S. and Datta, T.K. (2005), "Control of suspension bridge flutter instability using pole-placement technique", *J. Sound Vib.*, **282**, 89-109.
- Preumont, A. (1996), "Vibration control of active structures: An Introduction", Kluwer Academic publishers, 2nd Edn, SMIA.
- Shen, Y., Yang, S. and Yin, W. (2006), "Application of magnetorheological damper in vibration control of locomotive", *Proceedings of the 6th World Congress on Intelligent Control and Automation*, Dalian, China.
- Stefani, Shahian, Savant and Hostetter (2002), "Design of feedback control systems", Oxford University press.
- Yao, G.Z., Yap, F.F., Chen, G., Li, W.H. and Yeo, S.H. (2001), "MR damper and its application for semi-active control of vehicle suspension system", *Mechatronics*, **12**, 963-973.
- Ying, Z.G., Zhu, W.Q. and Soong, T.T. (2003) "A stochastic optimal semi-active control strategy for ER/MR dampers", *J. Sound Vib.*, **259**(1), 45-62.
- Yoshioka, H. and Murai N. (1999), "Active micro-vibration control system by pole assignment method using genetic algorithm", *Proceedings of SPIE -- Volume 3668, Smart Structures and Materials: Smart Structures and Integrated Systems*, 980-986.
- Zhu, Changsheng (2005), "A disk-type magneto-rheological fluid damper for rotor system vibration control", *J. Sound Vib.*, **283**(3-5), 1051-1069.
- Zhu, W.Q., Luo, M. and Dong L. (2004), "Semi-active control of wind excited building structures using MR/ER dampers", *Probabilist. Eng. Mech.*, **19**, 279-285.